

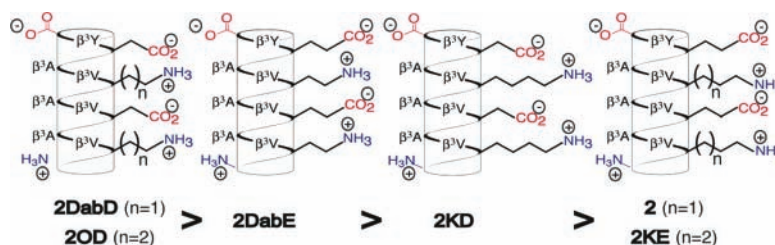
# Relationship between Salt-Bridge Identity and 14-Helix Stability of $\beta^3$ -Peptides in Aqueous Buffer

Danielle A. Guarracino,<sup>†</sup> HyoJin R. Chiang,<sup>‡</sup> Tereece N. Banks,<sup>†</sup> James D. Lear,<sup>§</sup> Michael E. Hodsdon,<sup>||</sup> and Alanna Schepartz<sup>\*,†,⊥</sup>

Departments of Chemistry, Molecular Biophysics and Biochemistry, and Molecular, Cellular and Developmental Biology, Yale University, New Haven, Connecticut 06520, Department of Biochemistry and Biophysics, School of Medicine, University of Pennsylvania, Philadelphia, Pennsylvania 19104, and Department of Laboratory Medicine, Yale School of Medicine, New Haven, Connecticut 06510  
alanna.schepartz@yale.edu

Received November 14, 2005

## ABSTRACT



We report a systematic analysis of the relationship between salt bridge composition and 14-helix structure within a family of model  $\beta$ -peptides in aqueous buffer. We find an inverse relationship between side-chain length and the extent of 14-helix structure as judged by CD. Introduction of a stabilizing salt bridge pair within a previously reported  $\beta$ -peptide ligand for hDM2 led to changes in structure that were detectable by NMR.

$\beta$ -Peptides adopt a diverse array of secondary structures including a variety of helices, pleated-sheets, and tubes.<sup>1–5</sup>  $\beta$ -Peptides composed of  $\beta^3$ -amino acids often assemble into a unique helical form called the 14-helix that is characterized by a defined set of long-range hydrogen bonds and three distinct faces.<sup>6</sup> Although the majority of published work in

the  $\beta^3$ -peptide field describes molecules folded in organic solvents,<sup>5</sup> in 2001 Seebach and DeGrado reported independently that  $\beta^3$ -peptides containing an alternating pattern of oppositely charged side chains at positions  $i$  and  $i+3$  on two of three helical faces displayed moderate levels of 14-helix structure in aqueous buffer.<sup>7–9</sup> We subsequently demonstrated that the requirement for stabilizing salt bridges on two helical faces could be lifted by introducing side chains that stabilize the 14-helix macrodipole.<sup>10,11</sup> We established that  $\beta$ -peptide 14-helices stabilized in this way tolerate a vast

<sup>†</sup> Department of Chemistry, Yale University.

<sup>‡</sup> Department of Molecular Biophysics & Biochemistry, Yale University.

<sup>§</sup> Department of Biochemistry and Biophysics, University of Pennsylvania.

<sup>||</sup> Department of Laboratory Medicine, Yale School of Medicine.

<sup>⊥</sup> Department of Molecular, Cellular & Developmental Biology, Yale University.

(1) Seebach, D.; Matthews, J. L. *Chem. Commun.* **1997**, 21, 2015–2022.

(2) DeGrado, W. F.; Schneider, J. P.; Hamuro, Y. *J. Peptide Res.* **1999**, 54, 206–217.

(3) Cheng, R. P.; Gellman, S. H.; DeGrado, W. F. *Chem. Rev.* **2001**, 101, 3219–3232.

(4) Martinek, T. A.; Fulop, F. *Eur. J. Biochem.* **2003**, 270, 3657–3666.

(5) For a recent review, see: Seebach, D.; Beck, A. K.; Bierbaum, D. J. *Chem. Biodiversity* **2004**, 1, 1111–1239.

(6) Seebach, D.; Overhand, M.; Kuhnle, F. N. M.; Martinoni, B.; Oberer, L.; Hommel, U.; Widmer, H. *Helv. Chim. Acta* **1996**, 79, 913–941.

(7) Arvidsson, P. I.; Rueping, M.; Seebach, D. *Chem. Commun.* **2001**, 7, 649–650.

(8) Cheng, R. P.; DeGrado, W. F. *J. Am. Chem. Soc.* **2001**, 123, 5162–5163.

(9) Rueping, M.; Mahajan, Y. R.; Jaun, B.; Seebach, D. *Chem. Eur. J.* **2004**, 10, 1607–1615.

(10) Kritzer, J. A.; Tirado-Rives, J.; Hart, S. A.; Lear, J. D.; Jorgensen, W. L.; Schepartz, A. *J. Am. Chem. Soc.* **2005**, 127, 167–178.

array of proteinogenic side chains<sup>10</sup> and can be modified to generate molecules that bind with moderate affinity to the proteins hDM2<sup>12</sup> and HIV gp41.<sup>13</sup> Here, we describe experiments that identify the charged side chain partners that best stabilize the 14-helix as judged by circular dichroism (CD) spectroscopy. We demonstrate that  $\beta^3$ -peptides containing  $\beta^3$ -HAspartate and either (*S*)-2,4-Homodiaminobutyric acid ( $\beta^3$ -HDab, Figure 1) or  $\beta^3$ -Hornithine along one helical face

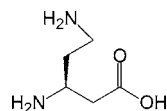


**Figure 1.** (*S*)-2,4-Homodiaminobutyric acid ( $\beta^3$ -HDab).

provide the greatest level of 14-helix stabilization. Introduction of the 14-helix stabilizing  $\beta^3$ -Hornithine/ $\beta^3$ -HAspartate salt bridge into the previously reported hDM2 ligand,  **$\beta$ 53-1**, led to changes in 14-helix structure that could be detected by 2D-NMR spectroscopy.

We studied a set of six  $\beta$ -dodecamers to evaluate the effect of side-chain identity on 14-helix stability in water (Figure 2). All six molecules are derivatives of the previously

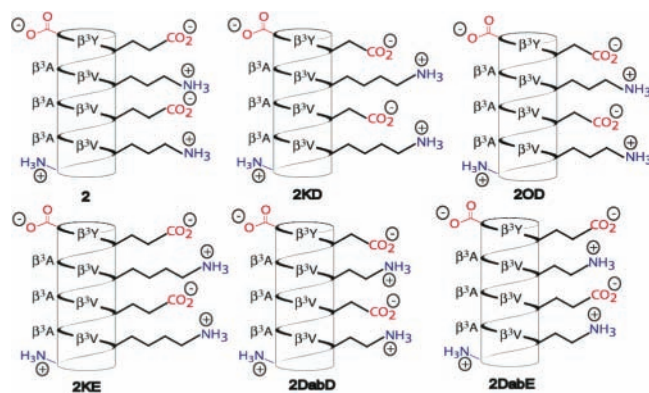


**Figure 2.** Helical net diagrams of  $\beta^3$ -peptides studied herein.

reported  $\beta$ -peptide **2**,<sup>10,11</sup> in which  $\beta^3$ -Hornithine (O) or  $\beta^3$ -HDab (Dab) replace  $\beta^3$ -HLysine (K) and  $\beta^3$ -HAspartate (D) replaces  $\beta^3$ -HGlutamate (E). All six  $\beta$ -dodecamers contain helix-promoting<sup>10,11,14</sup> aliphatic  $\beta^3$ -HValine residues at positions 2, 5, 8, and 11 along one face of the putative 14-helix and  $\beta^3$ -HALanine residues at positions 3, 6, and 9 along a second face. Each molecule also contained a  $\beta^3$ -HTyrosine

(11) Hart, S. A.; Bahadoor, A. B. F.; Matthews, E. E.; Qiu, X. Y. J.; Schepartz, A. *J. Am. Chem. Soc.* **2003**, *125*, 4022–4023.

(12) Kritzer, J. A.; Lear, J. D.; Hodsdon, M. E.; Schepartz, A. *J. Am. Chem. Soc.* **2004**, *126*, 9468–9469.

(13) Stephens, O. M.; Kim, S.; Welch, B. D.; Hodsdon, M. E.; Kay, M. S.; Schepartz, A. *J. Am. Chem. Soc.* **2005**, *127*, 13126–13127.

(14) Raguse, T. L.; Lai, J. R.; Gellman, S. H. *Helv. Chim. Acta* **2002**, *85*, 4154–4164.

residue to simplify spectrophotometric concentration determination. The  $\beta^3$ -peptides were synthesized using standard Fmoc solid-phase methods,<sup>15–17</sup> purified using reverse phase HPLC, and their sequences confirmed using MALDI-TOF mass spectrometry.<sup>18</sup> All six molecules are monomeric at 80  $\mu$ M as determined by analytical ultracentrifugation.

We used circular dichroism (CD) spectroscopy to monitor the extent of 14-helix structure in each  $\beta$ -peptide at 25 °C. While CD data on  $\beta$ -peptides must be interpreted carefully,<sup>19</sup> it is reasonable to assume that, for  $\beta^3$ -peptides in particular, changes in intensity of the 14-helical signature correlate to changes in 14-helical population.<sup>3,12,19,20</sup> The CD spectra of all six molecules are consistent with a 14-helix structure, with ellipticity minima between 211 and 214 nm, ellipticity maxima between 195 and 198 nm, and a crossover between negative and positive ellipticity between 200 and 202 nm (Figure 3a, Table 1).<sup>1,5,6</sup> The maximal values of negative

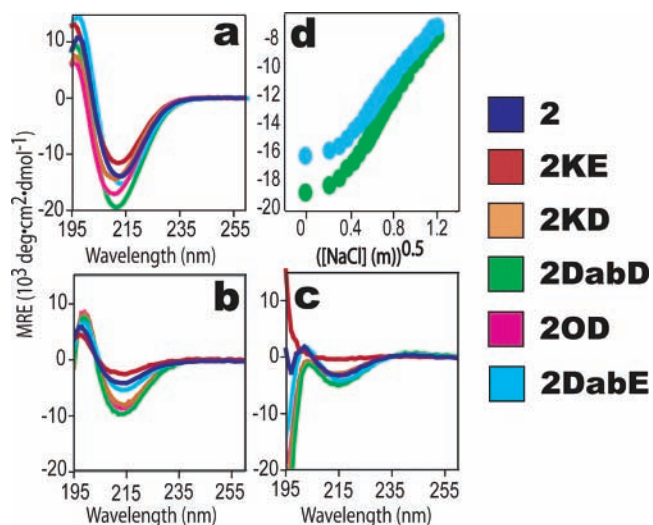


**Figure 3.** CD spectra of **2**, **2KE**, **2OD**, **2KD**, **2DabD**, **2DabE** at 80  $\mu$ M (PBC buffer) at: (a) pH 7 (b) pH 2 (c) pH 12. (d) MRE<sub>214</sub> of 100  $\mu$ M **2DabE** and **2DabD** vs [NaCl]<sup>0.5</sup>.

ellipticity range from  $-11500 \text{ deg}\cdot\text{cm}^2\cdot\text{dmol}^{-1}$  to  $-19500 \text{ deg}\cdot\text{cm}^2\cdot\text{dmol}^{-1}$ , representing a change of greater than 40%. The CD data suggest that the level of 14-helix structure among the six molecules is, from greatest to least: **2DabD** > **2OD** > **2DabE** > **2KD** > **2** > **2KE**.

**Table 1.** Minimum MRE ( $\text{deg}\cdot\text{cm}^2\cdot\text{dmol}^{-1}\cdot\text{residue}^{-1}$ ) for  $\beta$ -Peptides Studied Herein at 80  $\mu$ M and 25 °C

	$-\theta_{\min}$ (pH 7)	$-\theta_{\min}$ (pH 2)	$-\theta_{\min}$ (pH 12)	% $\Delta$ (pH 2/7)	% $\Delta$ (pH 12/7)
2DabD	19500	9690	4970	50	74
2OD	17100	8710	3370	49	80
2DabE	15200	5350	4110	65	73
2KD	14400	8040	2880	44	80
2	13900	4130	3190	70	77
2KE	11500	2570	376	78	97

Several trends emerge when the relative stabilities of the six  $\beta$ -peptides are compared. First, molecules containing  $\beta^3$ -HAsp display higher levels of 14-helix structure than otherwise identical molecules containing  $\beta^3$ -HGLu (compare **2DabD** vs **2DabE**, **2OD** vs **2**, and **2KD** vs **2KE**). Second, molecules containing  $\beta^3$ -HDab display higher levels of 14-helix structure than otherwise identical molecules containing  $\beta^3$ -HORN (compare **2DabD** vs **2OD**, and **2DabE** vs **2**). Finally, molecules containing  $\beta^3$ -HORN display higher levels of 14-helix structure than otherwise identical molecules containing  $\beta^3$ -HLys (compare **2OD** vs **2KD**, and **2** vs **2KE**). These trends suggest that the level of 14-helix structure in  $\beta$ -peptides related to **2** correlates inversely with side chain length: shorter side chains are better. Interestingly, solvent exposed salt bridges often contribute minimally to protein stability,<sup>21</sup> and glutamate, not aspartate, is the preferred partner for intra- $\alpha$ -helical salt bridges in proteins of known structure.<sup>22</sup>

The 14-helix stabilities of **2DabD** and **2DabE** were examined further by monitoring their CD spectra as a function of NaCl concentration at pH 7 in PBC buffer (Figure 3d). Both **2DabD** and **2DabE** become significantly less 14-helical as the NaCl concentration increases from 0 to 1.5 M as judged by the change in MRE<sub>214</sub>. In both cases the dependence of MRE<sub>214</sub> on NaCl concentration is approximately sigmoidal with a midpoint at 0.5 M NaCl; the plateaus observed at low salt suggest the formation of a stable conformation under these conditions. These CD data are highly reminiscent of those reported by DeGrado for a 15-residue  $\beta$ -peptide containing  $\beta^3$ -HLys/ $\beta^3$ -HGLu salt-bridges on two 14-helical faces and a C-terminal D-Asp; this molecule also showed a sigmoidal dependence of MRE<sub>214</sub> on NaCl concentration with a midpoint of 0.4 M NaCl.<sup>8</sup>

**$\beta$ 53-1**<sup>12</sup> is a structurally well-characterized<sup>23</sup>  $\beta$ -peptide that binds the oncoprotein hDM2 (Figure 4a). Based on the CD spectra of **2** and **2OD**, we hypothesized that substitution of  $\beta^3$ -HAsp for both  $\beta^3$ -HGLu residues in  **$\beta$ 53-1** would lead to differences in structure observable by NMR. As expected, the ROESY spectrum of  **$\beta$ 53-1D** at 10 °C in CD<sub>3</sub>OH showed multiple (ten of thirteen possible) long-range ROEs characteristic of the 14-helix conformation: five of seven possible C $\alpha$ H(*i*)  $\rightarrow$  C $\beta$ H(*i*+3) ROEs and five of six possible C<sub>N</sub>H(*i*)  $\rightarrow$  C $\beta$ H(*i*+3) ROEs (Figure 4b). Additional backbone ROEs

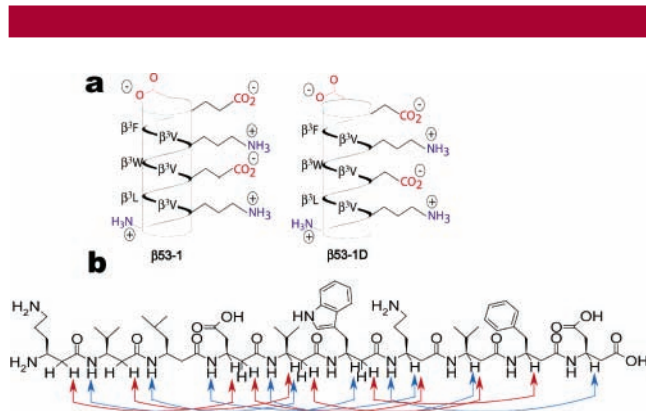


**Figure 4.** (a) Helical net diagrams depicting  **$\beta$ 53-1** and  **$\beta$ 53-1D**. (b) Backbone ROEs observed in the ROESY spectrum of  **$\beta$ 53-1D**; C $\alpha$ H(*i*)  $\rightarrow$  C $\beta$ H(*i*+3) ROEs are in red, C<sub>N</sub>H(*i*)  $\rightarrow$  C $\beta$ H(*i*+3) ROEs are in blue.

may have been present but were obscured by resonance overlap, as was true for  **$\beta$ 53-1**.<sup>12</sup> No backbone ROEs inconsistent with the 14-helix were observed. Overall, the ROESY spectrum of  **$\beta$ 53-1D** closely matched that of  **$\beta$ 53-1**, further supporting the conclusion that  **$\beta$ 53-1D** assembles into a 14-helix.

Interestingly, aliphatic <sup>13</sup>C-HSQC<sup>18</sup> and TOCSY<sup>24,25</sup> spectra revealed that the vicinal protons in the  $\gamma$  position of  $\beta^3$ -HORN at position 1 were clearly resolved in the NMR spectrum of  **$\beta$ 53-1D** but not  **$\beta$ 53-1** (Figure 5a,c). The portion

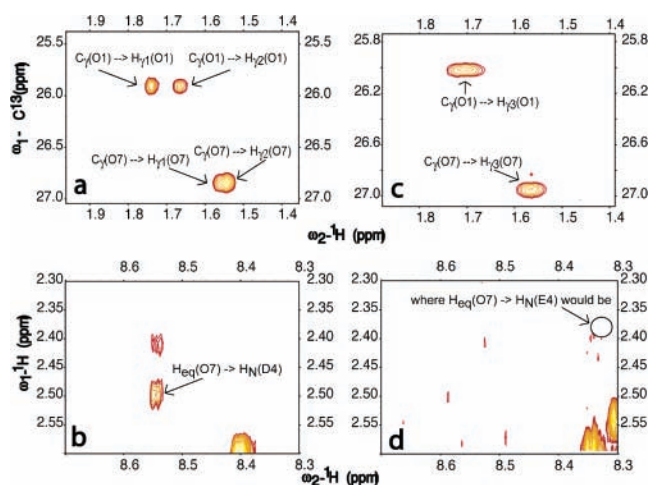


**Figure 5.** Differences in the 2D-NMR spectra of  **$\beta$ 53-1D** (a, b) and  **$\beta$ 53-1** (c, d). Regions of the <sup>13</sup>C-HSQC spectra are shown in a and c; differences in the ROESY spectra are shown in b and d.

of the aliphatic <sup>13</sup>C-HSQC NMR spectrum shown in Figure 5 identifies the interactions between the  $\gamma$  protons on  $\beta^3$ -HORN1 and 7 and the corresponding  $\gamma$  carbon within  **$\beta$ 53-**

(15) Rueping, M.; Jaun, B.; Seebach, D. *Chem. Commun.* **2000**, 22, 2267–2268.

(16) Guichard, G.; Abele, S.; Seebach, D. *Helv. Chim. Acta* **1998**, *81*, 187–206.

(17) Arvidsson, P. I.; Frackenpohl, J.; Seebach, D. *Helv. Chim. Acta* **2003**, *86*, 1522–1553.

(18) See the Supporting Information for details.

(19) Glattli, A.; Daura X.; Seebach, D.; van Gunsteren, W. F. *J. Am. Chem. Soc.* **2002**, *124*, 12972–12978.

(20) Park, J.-S.; Lee, H.-S.; Lai, J. R.; Kim, B. M.; Gellman, S. H. *J. Am. Chem. Soc.* **2003**, *125*, 8539–8545.

(21) (a) Iqbalsyah, T. M.; Doig, A. J. *Biochemistry* **2005**, *44*, 10449–10456. (b) Spek, E. J.; Bui, A. H.; Lu, M.; Kallenbach, N. R. *Protein Sci.* **1998**, *7*, 2431–2437. (c) Dao-pin, S.; Sauer, U.; Nicholson, H.; Matthews, B. W. *Biochemistry* **1991**, *30*, 7142–7153. (d) Horovitz, A.; Serrano, L.; Avron, B.; Bycroft, M.; Fersht, A. R. *J. Mol. Biol.* **1990**, *216*, 1031–1044.

(22) Sundaralingam, M.; Sekharudu, Y. C.; Yathindra, N.; Ravichandran, V. *Proteins* **1987**, *2*, 64–71.

(23) Kritzer, J. A.; Hodsdon, M. E.; Schepartz, A. *J. Am. Chem. Soc.* **2005**, *127*, 4118–4119.

(24) Rance, M. J. *Magn. Reson.* **1987**, *74*, 557–564.

(25) Braunschweiler, L.; E.; R. R. *J. Magnet. Res.* **1983**, *53*, 521–528.

**1D** (Figure 5a) and  **$\beta$ 53-1** (Figure 5c). In the case of  **$\beta$ 53-1**, the  $\gamma$  protons of both  $\beta^3$ -HOrn1 and 7 were broadened due to exchange and the exact positions of the two peaks could not be fully defined. In the case of  **$\beta$ 53-1D**, however, the  $\gamma$  protons of  $\beta^3$ -HOrn1 were narrower and resolved. The differences between  **$\beta$ 53-1D** and  **$\beta$ 53-1** were also seen in the ROESY spectra (Figure 5b,d). In the case of  **$\beta$ 53-1D**, we observed six long-range ROEs between protons on  $\beta^3$ -HOrn and those on proximal  $\beta^3$ -HAsp residue(s). These ROEs include three—those between protons of  $\beta^3$ -HAsp4 and  $\beta^3$ -HOrn7—that were not observed in the ROESY spectrum of  **$\beta$ 53-1** (Figure 5b,d). The ROESY spectra of  **$\beta$ 53-1D** and  **$\beta$ 53-1** also differed in terms of the distribution of long-range ROEs throughout the sequence: the spectrum of  **$\beta$ 53-1D** showed comparably fewer unambiguous ROEs between  $\beta^3$ -HOrn1 or  $\beta^3$ -HOrn7 and  $\beta^3$ -HAsp4 and 10 but comparably greater ROEs between  $\beta^3$ -HOrn7 and  $\beta^3$ -HAsp4. Overall, although the CD spectra of  **$\beta$ 53-1** and  **$\beta$ 53-1D** are nearly identical, the NMR data implies a subtle increase in the order of the salt-bridge side-chains in  **$\beta$ 53-1D** when compared with  **$\beta$ 53-1**.

In summary, here we provide evidence that salt bridge identity exerts an influence on 14-helix stability and identify the  $\beta^3$ -HDab/ $\beta^3$ -HAsp pair as the most stabilizing of those salt bridges studied. With this information in place, we can now apply the structure-stabilizing salt-bridge effects to the design of other biologically active  $\beta$ -peptides, thereby further assessing the delicate connection between  $\beta$ -peptide structure and function.

**Acknowledgment.** This work was supported by the NIH (GM65453 and GM74756), the National Foundation for Cancer Research, and in part by a grant to Yale University, in support of A.S., from the Howard Hughes Medical Institute.

**Supporting Information Available:**  $\beta^3$ -Peptide synthesis, purification, CD spectroscopy, and NMR spectroscopy. This material is available free of charge via the Internet at <http://pubs.acs.org>.

OL0527532